

Density dependent hadron field theory for neutron stars with antikaon condensates

Sarmistha Banik and Debades Bandyopadhyay

Saha Institute of Nuclear Physics, 1/AF Bidhannagar, Kolkata 700 064, India

Abstract

We investigate K^- and \bar{K}^0 condensation in β -equilibrated hyperonic matter within a density dependent hadron field theoretical model. In this model, baryon-baryon and (anti)kaon-baryon interactions are mediated by the exchange of mesons. Density dependent meson-baryon coupling constants are obtained from microscopic Dirac Brueckner calculations using Groningen and Bonn A nucleon-nucleon potential. It is found that the threshold of antikaon condensation is not only sensitive to the equation of state but also to antikaon optical potential depth. Only for large values of antikaon optical potential depth, K^- condensation sets in even in the presence of negatively charged hyperons. The threshold of \bar{K}^0 condensation is always reached after K^- condensation. Antikaon condensation makes the equation of state softer thus resulting in smaller maximum mass stars compared with the case without any condensate.

PACS: 26.60.+c, 21.65.+f, 97.60.Jd, 95.30.Cq

I. INTRODUCTION

The composition and structure of neutron stars depend on the nature of strong interaction. Neutron star matter encompasses a wide range densities, from the density of iron nucleus at the surface of the star to several times normal nuclear matter density in the core. Since the chemical potentials of nucleons and leptons increase rapidly with density in the interior of neutron stars, several novel phases of matter with large strangeness fraction such as, hyperonic matter, condensates of strange mesons and quark matter may appear there [1].

It was first demonstrated by Kaplan and Nelson within a chiral $SU(3)_L \times SU(3)_R$ model that K^- meson may undergo Bose-Einstein condensation in dense matter formed in heavy ion collisions [2]. In this model baryons directly couple with (anti)kaons. The effective mass of antikaons decreases with increasing density because of the strongly attractive K^- -baryon interaction in dense matter. Consequently, the in-medium energy of K^- mesons in the zero-momentum state also decreases with density. The s -wave K^- condensation sets in when the energy of K^- mesons equals to its chemical potential. Later, K^- condensation in the core of neutron stars was studied by other groups using chiral models [3].

Also, Bose-Einstein condensation of K^- mesons was investigated in the traditional meson exchange picture known as relativistic mean field (RMF) model [4–6]. Within the framework

of RMF model, baryon-baryon and (anti)kaon-baryon interactions are treated in the same footing i.e. those are mediated by the exchange of mesons [7–9]. It was noted in all these calculations that the typical threshold density of K^- condensation in nucleons-only neutron star matter was about $2-4n_0$, where n_0 is normal nuclear matter density. However, the threshold of antikaon condensation is sensitive to the antikaon optical potential and depends more strongly on the equation of state. With further inclusion of hyperons, K^- condensation was found to occur at higher densities [4–6,8,9]. Recently, we have studied \bar{K}^0 condensation along with K^- condensation in neutron stars using a relativistic mean field model and its influence on the structure of neutron stars [8,9]. The threshold density of \bar{K}^0 condensation is always higher than that of K^- condensation. Antikaon condensate makes the equation of state (EoS) softer, thus resulting in smaller maximum mass stars compared with the case without any condensate. Employing the EoS including both K^- and \bar{K}^0 condensates, it was predicted [9] that a stable sequence of superdense stars called the third family branch [10] might exist beyond the neutron star branch. The compact stars in the third family branch have smaller radii than those of the neutron star branch [9].

Besides EoS and antikaon optical potential depth, the threshold density of antikaon condensation is very much sensitive to the behaviour of antikaon energy and electron chemical potential at high density. The role of nucleon-nucleon and (anti)kaon-nucleon correlation on antikaon condensation were investigated by Pandharipande and collaborators [11,12]. They found that strong nucleon-nucleon and (anti)kaon-nucleon correlation raised the critical density for antikaon condensation to higher densities and predicted antikaon condensation might not be a possibility in neutron stars [12]. The electron chemical potential used in the above mentioned calculations was obtained from modern realistic nucleon-nucleon interactions [13,14].

In this work, we are interested to find out how many body correlations which may be taken into account by density dependent meson-baryon couplings in a relativistic field theoretical model, affect the threshold of antikaon condensation in neutron star matter. There is a growing interest to derive a quantum hadron field theory from a microscopic approach to nuclear interactions. The motivation of such an approach is not only to retain the essential features of quantum hadrodynamics (QHD) [15], but also to connect the complicated many body dynamics of strong interactions [16–18]. An appropriate and successful microscopic approach to in medium nuclear interactions follows from Dirac Brueckner (DB) calculations. Various groups performed DB calculations with realistic nucleon-nucleon interactions and reproduced empirical saturation properties of symmetric nuclear matter reasonably well [19–26]. Also nucleons-only neutron star matter was calculated in Dirac Brueckner theory [27–29]. It is worth mentioning here that the bulk of the screening of nucleon-nucleon interaction in medium is taken into account by the local baryon density dependent DB self energies [17]. This makes relativistic many body dynamics to be approximated by a density dependent relativistic hadron (DDRH) field theory [17,18]. A covariant and thermodynamically consistent DDRH field theory is obtained by making interaction vertices as Lorentz scalar functionals of baryon field operators. In the mean field approximation this model reduces to the relativistic Hartree description with density dependent meson-nucleon couplings. The density dependent meson-nucleon couplings are obtained from Dirac Brueckner self energies calculated with Bonn, Groningen and phenomenological density dependent potentials [30–35]. The variational derivatives of vertices with respect to baryon fields give rise

to rearrangement terms in baryon field equations [18]. Brockmann and Toki [16] first applied DDRH model without rearrangement terms to study finite nuclei. Recently, DDRH model with rearrangement terms has been exploited to investigate deformed nuclei [31], hypernuclei [33], asymmetric nuclear matter and exotic nuclei [34,35] and neutron star properties [36].

In this paper, we investigate antikaon condensation in beta equilibrated hyperon matter relevant to neutron stars and its role on the composition and structure of the compact stars in DDRH model. The paper is structured in the following way. In Sec. II, we describe DDRH model and different phases of matter. Parameters of the model are discussed in Sec. III. Results of our calculation are explained in Sec. IV. And Sec. V provides a summary and conclusions.

II. FORMALISM

Here, we discuss a phase transition from hadronic matter to antikaon condensed phase in compact stars. The hadronic phase is described within the framework of DDRH model. This phase is composed of all species of the baryon octet, electrons and muons. Therefore, the total Lagrangian density in the hadronic phase is written as $\mathcal{L} = \mathcal{L}_B + \mathcal{L}_l$. In DDRH model, baryon-baryon interaction is given by the Lagrangian density (\mathcal{L}_B) [36],

$$\begin{aligned} \mathcal{L}_B = & \sum_B \bar{\psi}_B \left(i\gamma_\mu \partial^\mu - m_B + g_{\sigma B} \sigma - g_{\omega B} \gamma_\mu \omega^\mu - \frac{1}{2} g_{\rho B} \gamma_\mu \boldsymbol{\tau}_B \cdot \boldsymbol{\rho}^\mu + \frac{1}{2} g_{\delta B} \boldsymbol{\tau}_B \cdot \boldsymbol{\delta} \right) \psi_B \\ & + \frac{1}{2} \left(\partial_\mu \sigma \partial^\mu \sigma - m_\sigma^2 \sigma^2 \right) + \frac{1}{2} \left(\partial_\mu \delta \partial^\mu \delta - m_\delta^2 \delta^2 \right) - \frac{1}{4} \omega_{\mu\nu} \omega^{\mu\nu} \\ & + \frac{1}{2} m_\omega^2 \omega_\mu \omega^\mu - \frac{1}{4} \boldsymbol{\rho}_{\mu\nu} \cdot \boldsymbol{\rho}^{\mu\nu} + \frac{1}{2} m_\rho^2 \boldsymbol{\rho}_\mu \cdot \boldsymbol{\rho}^\mu, \end{aligned} \quad (1)$$

and

$$\mathcal{L}_l = \sum_l \bar{\psi}_l (i\gamma_\mu \partial^\mu - m_l) \psi_l. \quad (2)$$

The field strength tensors for vector mesons are given by

$$\begin{aligned} \omega^{\mu\nu} &= \partial^\mu \omega^\nu - \partial^\nu \omega^\mu \\ \rho^{\mu\nu} &= \partial^\mu \rho^\nu - \partial^\nu \rho^\mu \end{aligned} \quad (3)$$

Here baryons are represented by Dirac spinors ψ_B (the index B denotes n, p, Λ , Σ^+ , Σ^- , Σ^0 , Ξ^- , Ξ^0), ψ_l ($l \equiv e, \mu$) is lepton spinor and $\boldsymbol{\tau}_B$ is isospin operator. The interactions among baryons are mediated by the exchange of σ , ω and ρ mesons. In addition to these mesons the scalar-isovector meson δ is also included. And this is important for an asymmetric system. Though the structure of DDRH Lagrangian density closely follows that of RMF model, there are important differences between those models. In RMF calculations with density independent meson-baryon coupling constants, non-linear self interaction terms for scalar and vector fields are inserted to account for higher order density dependent contributions. But this is not needed here as meson-baryon vertices $g_{\alpha B}$, where α denotes σ , ω , ρ and δ fields, are dependent on Lorentz scalar functionals of baryon field operators and adjusted to the Dirac-Brueckner-Hartree-Fock (DBHF) calculations [34,36].

We consider meson-baryon couplings $g_{\alpha B}(\hat{\rho})$ to depend on vector density. The density operator $\hat{\rho}$ has the form, $\hat{\rho} = \sqrt{\hat{j}_\mu \hat{j}^\mu}$, where $\hat{j}_\mu = \bar{\psi} \gamma_\mu \psi$. In the mean field approximation the operator $\hat{\rho}$ is replaced by ground state expectation value ρ i.e. $\langle \hat{\rho} \rangle = \rho$. Hence meson-baryon vertices become function of total baryon density in the hadronic phase,

$$\langle g_{\alpha B}(\hat{\rho}) \rangle = g_{\alpha B}(\langle \hat{\rho} \rangle) = g_{\alpha B}(\rho). \quad (4)$$

This is known as vector density dependence of vertices [17,34,36].

As vertices $g_{\alpha B}$ s are Lorentz scalar functional of baryon field operators, the variation of \mathcal{L} with respect to $\bar{\psi}_B$ gives,

$$\frac{\delta \mathcal{L}}{\delta \bar{\psi}_B} = \frac{\partial \mathcal{L}}{\partial \bar{\psi}_B} + \frac{\partial \mathcal{L}}{\partial \hat{\rho}_B} \frac{\delta \hat{\rho}_B}{\delta \bar{\psi}_B} \quad (5)$$

The rearrangement term $\Sigma^{\mu(r)} = \sum_B \frac{\partial \mathcal{L}}{\partial \hat{\rho}_B} \frac{\delta \hat{\rho}_B}{\delta \bar{\psi}_B}$ which originates from the second term of Eq. (5), naturally introduces additional contribution to vector self-energy [17,18,34,36]. This is an important difference between RMF and DDRH theory. The total vector self energy for baryon B in the hadronic phase is

$$\Sigma_{B,h}^\mu = \Sigma_{B,h}^{\mu(0)} + \Sigma_h^{\mu(r)}. \quad (6)$$

In the mean field approximation (MFA) adopted here, meson fields are replaced by their expectation values. Only the time-like components of vector fields, and isospin 3-components of ρ and δ fields have non-vanishing values in a uniform and static matter. The mean meson fields are denoted by σ , ω_0 , ρ_{03} and δ . Now the usual vector self energy is

$$\Sigma_{B,h}^{0(0)} = g_{\omega B} \omega_0 + \frac{1}{2} g_{\rho B} \tau_{3B} \rho_{03}. \quad (7)$$

Also, the rearrangement term simplifies to

$$\Sigma_h^{0(r)} = \sum_B \left[-\frac{\partial g_{\sigma B}}{\partial \rho_B} \sigma n_B^{s,h} + \frac{\partial g_{\omega B}}{\partial \rho_B} \omega_0 n_B^h + \frac{1}{2} \frac{\partial g_{\rho B}}{\partial \rho_B} \tau_{3B} \rho_{03} n_B^h - \frac{1}{2} \frac{\partial g_{\delta B}}{\partial \rho_B} \tau_{3B} \delta n_B^{s,h} \right], \quad (8)$$

where τ_{3B} is the isospin projection of baryon B and scalar and vector densities of baryon B in the hadronic phase are

$$\begin{aligned} n_B^{s,h} &= \langle \bar{\psi}_B \psi_B \rangle = \frac{2J_B + 1}{2\pi^2} \int_0^{k_{FB}} \frac{m_B^*}{(k^2 + m_B^{*2})^{1/2}} k^2 dk \\ &= \frac{m_B^*}{2\pi^2} \left[k_{FB} \sqrt{k_{FB}^2 + m_B^{*2}} - m_B^{*2} \ln \frac{k_{FB} + \sqrt{k_{FB}^2 + m_B^{*2}}}{m_B^*} \right], \end{aligned} \quad (9)$$

$$n_B^h = \langle \bar{\psi}_B \gamma_0 \psi_B \rangle = \frac{k_{FB}^3}{3\pi^2}. \quad (10)$$

Similarly, the expression of scalar self energy for baryon B is given by

$$\Sigma_{B,h}^s = g_{\sigma B} \sigma + \frac{1}{2} g_{\delta B} \tau_{3B} \delta. \quad (11)$$

One can immediately define baryon effective mass as $m_B^* = m_B - \Sigma_B^{s,h}$. And this differs for members of isospin multiplets due to δ meson. The rearrangement self energy modifies the baryon field equation compared to the RMF case [15],

$$[\gamma_\mu (i\partial^\mu - \Sigma_{B,h}^0) - (m_B - \Sigma_{B,h}^s)]\psi_B = 0. \quad (12)$$

To obtain the EoS of the pure hadronic phase, the equations of motion for baryons and mesons are solved self-consistently along with baryon effective mass in the mean field approximation keeping into consideration other constraints. The system is charge neutral and the condition of β -equilibrium is maintained. The charge neutrality condition is

$$Q^h = \sum_B q_B n_B^h - n_e - n_\mu = 0, \quad (13)$$

where q_B and n_B^h are electric charge and the number density of baryon B in the pure hadronic phase, respectively and n_e and n_μ are number densities of electrons and muons respectively. In compact star interior, chemical equilibrium is maintained through weak interactions such as $B_1 \rightarrow B_2 + l + \bar{\nu}_l$ and $B_2 + l \rightarrow B_1 + \nu_l$ where B_1 and B_2 are baryons and l stands for leptons. Therefore the generic equation relating chemical potentials for the above mentioned generalised β -decay processes is

$$\mu_B = b_B \mu_n - q_B \mu_e, \quad (14)$$

Here b_B is the baryon number of baryon B and μ_e is the chemical potential of electron. The chemical potential of baryon B in the hadronic phase is expressed as

$$\mu_B = \sqrt{k_{F_B}^2 + m_B^{*2}} + \Sigma_{B,h}^{0(0)} + \Sigma_h^{0(r)}. \quad (15)$$

It is noted that unlike RMF model, the rearrangement term appears in the expression of baryon chemical potential in DDRH model. In neutron stars, electrons are converted to muons by $e^- \rightarrow \mu^- + \bar{\nu}_\mu + \nu_e$ when the electron chemical potential becomes equal to the muon mass. Therefore, we have $\mu_e = \mu_\mu$ in compact stars. The above equation implies that there are two independent chemical potentials μ_n and μ_e corresponding to two conserved charges i.e. baryon number and electric charge. The energy density (ε^h) is related to the pressure (P^h) in this phase through the Gibbs-Duhem relation

$$P^h = \sum_i \mu_i n_i - \varepsilon^h. \quad (16)$$

Here μ_i and n_i are chemical potential and number density for i -th species. The expression of energy density in the hadronic phase is

$$\begin{aligned} \varepsilon^h = & \frac{1}{2} m_\sigma^2 \sigma^2 + \frac{1}{2} m_\omega^2 \omega_0^2 + \frac{1}{2} m_\rho^2 \rho_{03}^2 + \frac{1}{2} m_\delta^2 \delta^2 \\ & + \sum_B \frac{2J_B + 1}{2\pi^2} \int_0^{k_{F_B}} (k^2 + m_B^{*2})^{1/2} k^2 dk + \sum_l \frac{1}{\pi^2} \int_0^{K_{F_l}} (k^2 + m_l^2)^{1/2} k^2 dk. \end{aligned} \quad (17)$$

The rearrangement term does not contribute to the energy density explicitly, whereas it occurs in the pressure through baryon chemical potential. It is the rearrangement term

that accounts for the energy-momentum conservation and thermodynamic consistency of the system [18].

The pure antikaon condensed phase is composed of baryons, leptons and antikaons which are in chemical equilibrium under weak interactions and maintain local charge neutrality. The baryon-baryon interactions here are described by the Lagrangian density of DDRH model. It is worth mentioning here that the meson-baryon couplings depend on the total baryon density in this phase. In this phase, baryons are embedded in antikaon condensates. Earlier it was noted that baryons in the pure hadronic and antikaon condensed phase behaved differently because of their dynamical nature [7–9]. It was attributed to different mean fields which baryons experienced in those pure phases. We adopt here a relativistic field theoretical approach for the description of (anti)kaon-baryon interaction [7,9]. In this model (anti)kaon-baryon interactions are mediated by σ , ω , ρ and δ meson. The Lagrangian density for (anti)kaon interaction in the minimal coupling scheme is,

$$\mathcal{L}_K = D_\mu^* \bar{K} D^\mu K - m_K^{*2} \bar{K} K , \quad (18)$$

where the covariant derivative $D_\mu = \partial_\mu + ig_{\omega K} \omega_\mu + ig_{\rho K} \boldsymbol{\tau}_K \cdot \boldsymbol{\rho}_\mu / 2$. The isospin doublet for kaons is denoted by $K \equiv (K^+, K^0)$ and that for antikaons is $\bar{K} \equiv (K^-, \bar{K}^0)$. It is to be noted that the coupling constants of (anti)kaon-baryon interactions are considered to be density independent. The effective mass of (anti)kaons in this minimal coupling scheme is given by

$$m_K^* = m_K - g_{\sigma K} \sigma - \frac{1}{2} g_{\delta K} \tau_{3\bar{K}} \delta , \quad (19)$$

where m_K is the bare kaon mass. Here also the effective mass of K^- and \bar{K}^0 differ due to the inclusion of the scalar-isovector δ meson. The dispersion relation representing the in-medium energies of $\bar{K} \equiv (K^-, \bar{K}^0)$ for s -wave ($\mathbf{k} = 0$) condensation is given by

$$\omega_{K^-, \bar{K}^0} = m_K^* - g_{\omega K} \omega_0 \mp \frac{1}{2} g_{\rho K} \rho_{03} , \quad (20)$$

where the isospin projection $\tau_{3\bar{K}} = \mp 1$ for the mesons K^- ($-$ sign) and \bar{K}^0 ($+$ sign) are explicitly written in the expression. For s -wave condensation, densities of antikaons are given by

$$n_{K^-, \bar{K}^0} = 2 \left(\omega_{K^-, \bar{K}^0} + g_{\omega K} \omega_0 \pm \frac{1}{2} g_{\rho K} \rho_{03} \right) \bar{K} K = 2m_K^* \bar{K} K . \quad (21)$$

In the mean field approximation, the meson field equations in the presence of antikaon condensates are given by

$$m_\sigma^2 \sigma = \sum_B g_{\sigma B} n_B^{\bar{K}, s} + g_{\sigma K} \sum_{\bar{K}} n_{\bar{K}} , \quad (22)$$

$$m_\omega^2 \omega_0 = \sum_B g_{\omega B} n_B^{\bar{K}} - g_{\omega K} \sum_{\bar{K}} n_{\bar{K}} , \quad (23)$$

$$m_\rho^2 \rho_{03} = \frac{1}{2} \sum_B g_{\rho B} \tau_{3B} n_B^{\bar{K}} + \frac{1}{2} g_{\rho K} \sum_{\bar{K}} \tau_{3\bar{K}} n_{\bar{K}} , \quad (24)$$

$$m_\delta^2 \delta = \frac{1}{2} \sum_B g_{\delta B} \tau_{3B} n_B^{\bar{K}, s} + \frac{1}{2} g_{\delta K} \sum_{\bar{K}} \tau_{3\bar{K}} n_{\bar{K}} , \quad (25)$$

where $n_B^{\bar{K},s}$ and $n_B^{\bar{K}}$ are scalar and vector density of baryon B in the antikaon condensed phase and have the same forms as in Eqs. (9) and (10). The meson field equations here remain same in structure as RMF ones [7–9], but the constant meson-baryon couplings are replaced by their density dependent counterparts.

The total energy density and pressure in the antikaon condensed phase are given by

$$\begin{aligned} \varepsilon^{\bar{K}} = & \frac{1}{2}m_\sigma^2\sigma^2 + \frac{1}{2}m_\omega^2\omega_0^2 + \frac{1}{2}m_\rho^2\rho_{03}^2 + \frac{1}{2}m_\delta^2\delta^2 \\ & + \sum_B \frac{2J_B + 1}{2\pi^2} \int_0^{k_{FB}} (k^2 + m_B^{*2})^{1/2} k^2 dk + \sum_l \frac{1}{\pi^2} \int_0^{K_{Fl}} (k^2 + m_l^2)^{1/2} k^2 dk \\ & + m_K^* (n_{K^-} + n_{\bar{K}^0}) , \end{aligned} \quad (26)$$

and

$$\begin{aligned} P = & -\frac{1}{2}m_\sigma^2\sigma^2 + \frac{1}{2}m_\omega^2\omega_0^2 + \frac{1}{2}m_\rho^2\rho_{03}^2 - \frac{1}{2}m_\delta^2\delta^2 + \Sigma_{\bar{K}}^{0(r)} \sum_B n_B^{\bar{K}} \\ & + \frac{1}{3} \sum_B \frac{2J_B + 1}{2\pi^2} \int_0^{k_{FB}} \frac{k^4 dk}{(k^2 + m_B^{*2})^{1/2}} + \frac{1}{3} \sum_l \frac{1}{\pi^2} \int_0^{K_{Fl}} \frac{k^4 dk}{(k^2 + m_l^2)^{1/2}} , \end{aligned} \quad (27)$$

where $\Sigma_{\bar{K}}^{0(r)}$ is the rearrangement term in the antikaon condensed phase and has the same form as in Eq. (8), but all quantities in the equation are replaced by the corresponding quantities of the antikaon condensed phase. Since antikaons form s-wave condensates, they do not contribute to the pressure directly. Actually the effect of antikaons in the pressure term comes through the meson fields.

In the core of neutron stars, various strangeness changing processes may occur such as $N \rightleftharpoons N + \bar{K}$ and $e^- \rightleftharpoons K^- + \nu_e$, where $N \equiv (n, p)$ and $\bar{K} \equiv (K^-, \bar{K}^0)$ denote the isospin doublets for nucleons and antikaons, respectively. From the above reactions in chemical equilibrium, we obtain the conditions for antikaon condensation

$$\mu_n - \mu_p = \mu_{K^-} = \mu_e , \quad (28)$$

$$\mu_{\bar{K}^0} = 0 , \quad (29)$$

where μ_{K^-} and $\mu_{\bar{K}^0}$ are respectively the chemical potentials of K^- and \bar{K}^0 . The charge neutrality condition in the antikaon condensed phase is

$$Q^{\bar{K}} = \sum_B q_B n_B^{\bar{K}} - n_{K^-} - n_e - n_\mu = 0. \quad (30)$$

It was noted in RMF model calculations that antikaon condensation could be either first order or second order phase transition depending on the parameter set of the model and antikaon optical potential depth [7–9]. If the phase transition is of first order, the mixed phase is to be determined by the Gibbs conditions and global baryon and electric charge conservation laws because we have conserved baryon and electric charges represented by two chemical potentials μ_n and μ_e [37]. The Gibbs phase rules read,

$$P^h = P^{\bar{K}}, \quad (31)$$

$$\mu_B^h = \mu_B^{\bar{K}}, \quad (32)$$

where μ_B^h and $\mu_B^{\bar{K}}$ are chemical potentials of baryon B in the pure hadronic and K^- condensed phase, respectively. The conditions of global charge neutrality and baryon number conservation are imposed through the relations

$$(1 - \chi)Q^h + \chi Q^{\bar{K}} = 0, \quad (33)$$

$$n_B = (1 - \chi)n_B^h + \chi n_B^{\bar{K}}, \quad (34)$$

where χ is the volume fraction of K^- condensed phase in the mixed phase. The total energy density in the mixed phase is

$$\epsilon = (1 - \chi)\epsilon^h + \chi\epsilon^{\bar{K}}. \quad (35)$$

III. PARAMETERS

A. Meson-nucleon couplings

In DDRH model, meson-nucleon vertices are obtained from microscopic DB calculations of symmetric and asymmetric nuclear matter. The density dependent vertices in the RMF model are related to DB self energies in the local density approximation [16,30]. Equating self-energies of infinite nuclear matter in RMF and DB calculations, we obtain

$$\Sigma^{RMF} = g_\alpha \phi_\alpha = \Sigma^{DB}, \quad (36)$$

where ϕ_α represents the field for α meson. Putting the value of ϕ_α as given by the meson field equations in the presence of nucleons, the above relation simplifies to

$$m^2 \Sigma^{DB} = g_\alpha^2 n_\alpha \quad (37)$$

where n_α is the density corresponding to ϕ_α field. Scalar and vector self energies for neutrons and protons were obtained in DB calculations of asymmetric nuclear matter using Groningen potential [26,38,39]. Using these values of Σ^{DB} , one immediately obtains the density dependent meson-baryon couplings [34]. A suitable parameterization for density dependent couplings was made in Ref. [34]. It has the form

$$g_\alpha(\rho) = a_\alpha \frac{1 + b_\alpha(\rho/\rho_0 + d_\alpha)^2}{1 + c_\alpha(\rho/\rho_0 + e_\alpha)^2} \quad (38)$$

where $\rho_0 = 0.16 \text{ fm}^{-3}$ and parameters of the fit are listed in Table I of Ref. [34]. However, the results of infinite nuclear matter calculation in DDRH model using the above mentioned parameterization deviated from those of DB calculations [34]. Therefore, momentum dependent vertices with the additional constraint that the energy density in DB and DDRH are same i.e. $\epsilon^{DB} = \epsilon^{DDRH}$ was proposed [34]. Momentum corrected meson-nucleon vertices are given by

$$\tilde{g}_\alpha(k_F) = g_\alpha(k_F) \sqrt{1 + \zeta_\alpha k_F^2} = \tilde{\zeta}_\alpha(k_F) g_\alpha(k_F), \quad (39)$$

with $\zeta_\sigma=0.00804 \text{ fm}^2$ and $\zeta_\omega=0.00103 \text{ fm}^2$ as calculated in Ref. [34]. Using the momentum corrected vertices, Dirac Brueckner EoS for symmetric matter was reproduced well [34]. Also, momentum correction was incorporated in ρ -meson-nucleon vertex and the parameters of Eq.(38) after momentum correction are given by Table II in Ref. [34]. We adopt this parameterization of density dependent couplings and the momentum correction prescription in our calculation. Also, we denote this as Groningen parameter set. In Table I, we show meson-baryon couplings for Groningen set at saturation density ($n_0 = 0.18 \text{ fm}^{-3}$). The momentum correction modifies the rearrangement term as $\frac{\partial g_{\alpha B}}{\partial \rho}$ is to be replaced by $\frac{\partial \tilde{g}_{\alpha B}}{\partial \rho}$; this is given by [34]

$$\frac{\partial \tilde{g}_{\alpha B}(k_F)}{\partial \rho} = \tilde{\zeta}_\alpha(k_F) \frac{\partial g_{\alpha B}(k_F)}{\partial \rho} + \frac{\zeta_\alpha k_F^2 g_\alpha(k_F)}{3\rho \tilde{\zeta}_{\alpha B}(k_F)}. \quad (40)$$

In this calculation, we also exploit density dependent meson-nucleon vertices obtained from DB calculations using Bonn A potential. The parameterization of vertices is taken from Ref. [30]. This parameter set is denoted as Bonn A parameter set. For Bonn A set, ρ meson-nucleon coupling is chosen as a constant. Also, δ meson is not taken into consideration for Bonn A potential. Meson-nucleon coupling constants at saturation density $n_0 = 0.159 \text{ fm}^{-3}$ are listed in Table I.

B. Meson-hyperon couplings

In the absence of DB calculation including hyperons, density dependence of meson-hyperon vertices are obtained from density dependent meson-nucleon couplings using hypernuclei data [5] and scaling law [33]. This scaling law states that the self energies and vertices of hyperons and nucleons are related to each other by their free space coupling constants $\bar{g}_{\sigma Y}$ and $\bar{g}_{\sigma N}$.

$$R_{\alpha Y} = \frac{g_{\alpha Y}}{g_{\alpha N}} \simeq \frac{\Sigma_{\alpha Y}}{\Sigma_{\alpha N}} \simeq \frac{\bar{g}_{\alpha Y}}{\bar{g}_{\alpha N}}. \quad (41)$$

In RMF model, vector meson-hyperon coupling constants were determined from scaling factors obtained from SU(6) symmetry relations of the quark model [5,40]. Another possibility is to exploit scaling factors calculated in microscopic calculations. However, there is only one microscopically derived free space scaling factor $R_{\sigma\Lambda}=0.49$ in the literature [41]. We use this value in our calculation. Also, we obtain the scaling factors for vector and isovector mesons from SU(6) symmetry relations,

$$\begin{aligned} \frac{1}{2}g_{\omega\Sigma} &= g_{\omega\Xi} = \frac{1}{3}g_{\omega N}, \\ \frac{1}{2}g_{\rho\Sigma} &= g_{\rho\Xi} = g_{\rho N}; \quad g_{\rho\Lambda} = 0, \\ \frac{1}{2}g_{\delta\Sigma} &= g_{\delta\Xi} = g_{\delta N}; \quad g_{\delta\Lambda} = 0. \end{aligned} \quad (42)$$

We obtain $g_{\omega\Lambda}$ and scalar meson couplings to other hyperons from the potential depth of a hyperon in normal nuclear matter. And in DDRH model, it is given by

$$U_Y^N = \Sigma_Y^{0(0)} + \Sigma_N^{0(r)} - \Sigma_Y^s, \quad (43)$$

where $\Sigma_Y^{0(0)} = g_{\omega Y}\omega_0$, $\Sigma_Y^s = g_{\sigma Y}\sigma$ and $\Sigma_N^{0(r)}$ is the rearrangement contribution of nucleons. In this calculation, the value of Λ potential in normal nuclear matter is taken as -30 MeV [40,42] and that of Ξ is -18 MeV [43,44]. The most updated analysis of Σ^- atomic data [45] and other experimental data [46] predict a repulsive Σ -nucleus potential depth. Therefore, we adopt a Σ well depth of 30 MeV in this calculation [46]. We find that Σ hyperons are excluded from the system because of this repulsive potential. The scaling factors of Λ and Ξ for Groningen and Bonn A potential are listed in Table 2.

C. Meson-(anti)kaon coupling constants

Finally, we need to determine the parameter set for meson-(anti)kaon interactions. Here, We do not attribute any density dependence to the vertices of meson-(anti)kaons. The vector coupling constants are derived from quark model and isospin counting rule so that

$$g_{\omega K} = \frac{1}{3}g_{\omega N} \quad \text{and} \quad g_{\rho K} = g_{\rho N}. \quad (44)$$

The values of meson-nucleon coupling constants are taken at normal nuclear matter density and those are given by Table I. The scalar coupling constant is obtained from the real part of K^- optical potential at normal nuclear matter density

$$U_{\bar{K}}(n_0) = -g_{\omega K}\omega_0 - g_{\sigma K}\sigma + \Sigma_N^{0(r)}. \quad (45)$$

The scalar isovector δ meson also couples with (anti)kaons. The coupling of δ meson with (anti)kaons is obtained from simple quark model and this is given by $g_{\delta K} = g_{\delta N}$. The value of $g_{\delta N}$ is obtained from Table I.

There are experimental evidences that antikaons experience an attractive interaction whereas kaons feel a repulsive interaction in nuclear matter [47,48]. It is the depth of antikaon optical potential which is an important input in our calculation. The real part of antikaon optical potential at normal nuclear matter density was evaluated in coupled channel model [49,50] and self consistent calculations [51–53]. These model calculations give a wide range of values from -120 MeV to -40 MeV for $U_{\bar{K}}$ at n_0 . Recently, a combined chiral analysis of K^- atomic and K^-p scattering data lead to a shallow attractive $U_{\bar{K}}(n_0)$ of -55 MeV [54]. On the other hand, the analysis of K^- atomic data in the hybrid model [55] yielded $U_{\bar{K}}(n_0) = -180 \pm 20$ MeV. Therefore, there is no consensus among the phenomenological and microscopic potentials both in terms of depth and χ^2 values. The coupling constants for kaons with σ -meson, $g_{\sigma K}$, for a set values of $U_{\bar{K}}$ from -120 MeV to -180 MeV at saturation density for Groningen and Bonn A potential are listed in Table 3.

IV. RESULTS AND DISCUSSION

Here we report the results of our calculation in DDRH model using Groningen set. We perform this calculation for antikaon optical potential $U_{\bar{K}}(n_0) = -120$ to -180 MeV. There is no \bar{K} condensation as a first order phase transition for Groningen set and various

values of $U_{\bar{K}}(n_0)$. Rather, K^- and \bar{K}^0 condensation are second order phase transitions in this calculation. In this situation, the conditions of antikaon condensation are given by Eqs. (28) and (29). Earlier it was found in RMF calculations that antikaon condensation could be a second order phase transition depending on the antikaon optical potential and coupling constants of the models [7–9]. The threshold densities of K^- and \bar{K}^0 condensation in β -equilibrated matter containing n,p, Λ and leptons for $U_{\bar{K}}(n_0) = -120$ to -180 MeV are recorded in Table IV. Besides Λ hyperons, we also include other species of hyperons into our calculation. However, Σ hyperons do not appear because of a repulsive Σ -baryon interaction. In Table IV, the critical densities of \bar{K} condensation in β -equilibrated n,p, Λ , Ξ and lepton matter are given in the parentheses. The early appearance of hyperons might have important effect on the threshold densities of \bar{K} condensation because hyperons make the equation of state soft. It was shown in RMF model calculations that the onset of \bar{K} condensation was delayed to higher densities due to hyperons [4–6,8,9]. Also, negatively charged hyperons diminish the electron chemical potential delaying the onset of K^- condensation. In this DDRH model calculation with Groningen set, Λ hyperons appear first. Consequently, the threshold densities of \bar{K} condensation are shifted to higher densities compared with those in nucleons-only matter. With further appearance of negatively charged Ξ^- hyperons, K^- condensation occurs at higher densities as it is evident from the values in the parentheses in Table IV. For $U_{\bar{K}}(n_0) = -120$ MeV, the early appearance of Ξ^- completely blocks the onset of both K^- and \bar{K}^0 condensation even in the highest density ($8n_0$) considered in this calculation. On the other hand, the impact of Ξ^- hyperons on the threshold densities of \bar{K}^0 condensation for $|U_{\bar{K}}(n_0)| \geq 160$ MeV is negligible. This may be attributed to the fact that the density of Ξ^- hyperons falls after the onset of K^- condensation. This becomes evident when we discuss the particle fraction graphs in the following paragraphs. From Table IV, we note that the threshold density of \bar{K} condensation shifts towards lower density as the strength of $|U_{\bar{K}}(n_0)|$ increases. This indicates the threshold of \bar{K} condensation is not only dependent on the EoS, but also sensitive to antikaon optical potential depth. For all values of $U_{\bar{K}}(n_0)$, we observe K^- condensation occurs before \bar{K}^0 condensation.

The composition of neutron star matter containing nucleons (n,p), Λ hyperon, electron (e^-), muon (μ^-) and K^- and \bar{K}^0 mesons for Groningen set and $U_{\bar{K}}(n_0) = -160$ MeV is presented in Fig. 1. Before the onset of K^- condensation, the charge neutrality is maintained by protons, electrons and muons in the hadronic phase. We see that Λ hyperon is the first strange baryon to appear in the hadronic phase at $1.99n_0$, where $n_0 = 0.18 fm^{-3}$. Its density rises fast at the cost of neutrons. In this calculation, K^- condensation sets in at $2.65n_0$. As soon as K^- condensate appears, it rapidly grows and readily replaces e^- and μ^- . This behaviour is quite expected, as K^- mesons, being bosons, condense in the lowest energy state and are therefore energetically favorable to maintain charge neutrality of the system. The electron fraction depletes around $4.8n_0$ and the proton density becomes equal to that of K^- condensate. The appearance of \bar{K}^0 condensate is delayed to $6.16n_0$. With the onset of \bar{K}^0 condensation the abundances of n,p, K^- and \bar{K}^0 become identical leading to an isospin saturated symmetric matter. Here the system is dominated by Λ hyperons at high density. It is worth mentioning here that the results of DDRH model for Groningen set and $U_{\bar{K}}(n_0) = -160$ MeV resemble those of the RMF model for GM1 set and $U_{\bar{K}}(n_0) = -160$ MeV. However, antikaon condensation in the latter case was a first order phase transition.

Besides Λ hyperon formation, we also consider the role of other hyperons, such as Ξ^0 and

Ξ^- on antikaon condensation. In Fig. 2, we note that negatively charged Ξ^- hyperons start populating the system at $2.24n_0$, soon after the appearance of Λ . This further postpones K^- condensation to $3.20n_0$. Lepton fractions begin to fall with the onset of negatively charged Ξ^- . This is quite expected because it is energetically favourable to achieve charge neutrality among particles carrying conserved baryon numbers. No such conservation law is followed by leptons or mesons. But as soon as K^- condensation sets in, lepton fractions as well as Ξ^- fraction drop. It indicates that the EoS is now mainly softened by the presence of Λ hyperons and K^- condensate. This has an interesting implication on the threshold density of \bar{K}^0 condensation. It is evident from Table IV, \bar{K}^0 condensation occurs at same density point $6.16 n_0$ with and without the inclusion of Ξ^- in our calculation. Also, a symmetric matter of n,p, K^- and \bar{K}^0 condensate emerges here after the onset of \bar{K}^0 condensation. At a much higher density $6.7n_0$, Ξ^0 appears in the system.

Pressure (P) is plotted against energy density (ϵ) for various compositions of nuclear star matter in Fig. 3. Here equations of state (EoS) are calculated with Groningen set. The dotted line stands for nucleons-only matter, while the dash-dotted line contains Λ hyperons in addition to nucleons. The presence of an additional degree of freedom softens the EoS appreciably. The solid lines correspond to Λ hyperon matter including K^- and \bar{K}^0 condensate for antikaon optical potentials $U_{\bar{K}}(n_0) = -120$ to -180 MeV. The kinks on the equations of state mark the onsets of \bar{K} condensation. Already, we have noted that K^- and \bar{K}^0 condensation are second order phase transitions for all values of $U_{\bar{K}}(n_0)$ in our calculation. From Fig. 3, we find pressure increases with energy density even after the onset of antikaon condensation. The appearance of K^- condensate makes equations of state softer in all cases. The kinks at higher densities correspond to \bar{K}^0 condensation which further softens the EoS. Also, the softness in the EoS is very sensitive to antikaon optical potential depth. Stronger the attractive antikaon interaction, softer is the corresponding EoS.

The results of static structures of spherically symmetric neutron stars calculated using Tolman-Oppenheimer-Volkoff (TOV) equations [1] and the above mentioned equations of state are now presented here. We have used the results of Baym, Pethick and Sutherland [56] to describe the crust of a compact star composed of leptons and nuclei for the low density ($n_B < 0.001 fm^{-3}$) EoS. In the mid density regime ($0.001 \leq n_B < 0.08 fm^{-3}$) the results of Negele and Vautherin [57] are taken into account. Above this density, an EoS calculated in DDRH model has been adopted. The maximum neutron star masses (M_{max}/M_\odot) and their central densities ($u_{cent} = n_{cent}/n_0$) for various compositions of matter are listed in Table IV. The values recorded within the parentheses correspond to the calculations including Ξ hyperons in addition to Λ hyperons. The maximum mass of nucleons-only star is $2.313M_\odot$. The inclusion of Λ hyperons softens the EoS lowering this value to $1.708M_\odot$. Because of further softening due to the inclusion of Ξ hyperons the maximum mass is reduced to a value of $1.620M_\odot$. The static neutron star sequences representing the stellar masses M/M_\odot and the corresponding central energy densities (ϵ) are exhibited in Fig. 4 for n,p, Λ and lepton matter with K^- and \bar{K}^0 condensate and different values of $U_{\bar{K}}(n_0)$. The softening in the EoS due to the presence of \bar{K} condensates, leads to further lowering in the limiting masses of neutron stars that too attain at much earlier central densities as it is evident from Table IV. The maximum mass of the star varies from $1.697M_\odot$ (for $U_{\bar{K}}(n_0) = -120$ MeV) to $1.497M_\odot$ (for $U_{\bar{K}}(n_0) = -180$ MeV) because strong attractive antikaon interaction in medium produces

more softening in the EoS. For n,p, Λ , lepton and \bar{K} condensate matter composition, K^- condensation thresholds occur well inside the maximum mass stars for all values of $U_{\bar{K}}(n_0)$. So the star is mainly composed of nucleons, Λ hyperons and K^- condensate. On the other hand, \bar{K}^0 condensation along with K^- condensation might be a possibility in maximum mass neutron stars for $|U_{\bar{K}}(n_0)| \geq 180$ MeV.

We also inspect the effect of Ξ hyperons on the compact star mass sequence. Already we have discussed that the appearance of Ξ^- hyperons prevents the onset of \bar{K} condensation for $U_{\bar{K}}(n_0) = -120$ MeV. From Table IV, we find no \bar{K} condensation occurs inside the limiting mass neutron stars for $|U_{\bar{K}}(n_0)| \leq 140$ MeV. For these values of $U_{\bar{K}}(n_0)$, the maximum star mass is the same as that of the case without any antikaon condensate. On the other hand, K^- condensate is formed inside maximum mass stars for $|U_{\bar{K}}(n_0)| \geq 160$ MeV, but \bar{K}^0 condensation in neutron stars is ruled out for all values of $U_{\bar{K}}(n_0)$ except for antikaon potential depth of -180 MeV. For $|U_{\bar{K}}(n_0)| \geq 160$ MeV, we observe there is hardly any change in the maximum masses of neutron stars compared with the cases excluding Ξ hyperons. Already we have noted in the discussion of Fig. 2 that the density of Ξ^- hyperon diminishes with the appearance of K^- condensate for $|U_{\bar{K}}(n_0)| \geq 160$ MeV. Now we show the equations of state for neutron star matter with and without Ξ hyperons for $U_{\bar{K}}(n_0) = -160$ MeV in Fig. 5. The solid and dashed line represent neutron star matter with and without Ξ hyperons respectively. The EoS becomes softer in the presence of Ξ^- hyperons, but there is no difference between the equations of state just after the onset of K^- condensation. This feature is reflected in the maximum masses of neutron stars as is evident from Table IV.

In Fig. 6, we draw the mass-radius relationship for n,p, Λ , lepton and \bar{K} condensate matter in DDRH model using Groningen set and different antikaon optical potential depths and compare it with our previous result for hyperonic matter including K^- condensate calculated in the RMF model [9] using GM1 model and $U_{\bar{K}}(n_0) = -160$ MeV. The filled circles correspond to the maximum masses of compact stars. For $U_{\bar{K}}(n_0) = -120$ MeV, the maximum mass star has a radius 11.76 km, whereas it is 11.39 km for $U_{\bar{K}}(n_0) = -180$ MeV in DDRH model. The smaller radius in the latter case may be attributed to more softening in the EoS due to strong attractive antikaon potential. The curve corresponding to the RMF calculation [9] has the smallest radius of 10.9 km among all the cases considered here.

We also investigate K^- condensation in nucleons-only matter using Bonn A set as described in Table I and antikaon optical potential depth at normal nuclear matter density $U_{\bar{K}}(n_0) = -160$ MeV. For Bonn A set, σ -nucleon and ω -nucleon couplings are density dependent whereas ρ -nucleon coupling is a constant one. Here we study the EoS and structure of neutron stars. Unlike the situation with Groningen set, antikaon condensation in this case is a first order phase transition which is governed by Gibbs phase rules and global conservation laws as given by Eqs. (31)-(35). The EoS for nucleons-only matter with and without K^- condensate are denoted by dotted and solid line in Fig. 7 respectively. The kink on the dotted curve indicates the onset of antikaon condensation at $2.49n_0$, where $n_0 = 0.159 \text{ fm}^{-3}$. And the phase transition is over at $3.47n_0$. Those two points give the extent of the mixed phase. We have pure hadronic phase below the lower boundary and antikaon condensed phase above the upper boundary. It follows from the structure calculation using TOV equations, the maximum masses of nucleons-only stars with and without K^- condensate for Bonn A set are $2.55M_\odot$ and $2.32M_\odot$ having central densities 5.64 and $6.84 n_0$, respectively. In this case, we find the radii for neutron stars with and without K^- condensate are 10.88

km and 9.91 km, respectively. These values of maximum masses and radii in Bonn A set are smaller than those of Groningen set. Because of the behaviour of the parameterization of the couplings in the high density regime for Bonn A set, the repulsion due to ω field becomes larger than the attraction of σ field. Consequently, the EoS in Bonn A set is stiffer than that of Groningen set. A close inspection of the parameterization of couplings in Bonn A set has been already suggested in Ref. [31].

V. SUMMARY AND CONCLUSIONS

We have studied K^- and \bar{K}^0 condensation in β -equilibrated hyperonic matter within a density dependent hadron field theoretical model. In this model, baryon-baryon and (anti)kaon-baryon interactions are mediated by the exchange of σ , ω , ρ and δ meson. Density dependent meson-baryon coupling constants are obtained from microscopic Dirac Brueckner calculations using Groningen and Bonn A nucleon-nucleon potential. On the other hand, we have considered constant meson-(anti)kaon couplings in this calculation.

For Groningen set and the values of antikaon optical potential $U_{\bar{K}}(n_0) = -120$ to -180 MeV, both K^- and \bar{K}^0 condensation are found to be second order phase transition. The early appearance of Λ hyperons delays \bar{K} condensation to higher density for all values of $U_{\bar{K}}(n_0)$ considered here. With further inclusion of Ξ hyperons, K^- as well as \bar{K}^0 condensation do not occur at all for $|U_{\bar{K}}|(n_0) < 120$ MeV, whereas \bar{K} condensate appears after being delayed by Ξ hyperons for $|U_{\bar{K}}|(n_0) \geq 140$ MeV. It is interesting to note that as soon as K^- condensate appears in the system, the density of Ξ^- drops. It is found that antikaon condensation is not only sensitive to the equation of state but also to antikaon optical potential depth.

The equations of state for different neutron star matter compositions including \bar{K} condensate have been studied in DDRH model. The appearance of antikaon condensation makes the corresponding EoS softer. This softening leads to the reduction in maximum masses of neutron stars for different cases considered here. For different compositions of neutron star matter, it is observed that K^- condensation may occur in maximum mass stars but the appearance of \bar{K}^0 is ruled out except for $|U_{\bar{K}}(n_0)| \geq 180$ MeV. The neutron star with smallest maximum mass and radius is obtained for $U_{\bar{K}}(n_0) = -180$ MeV in DDRH model with Groningen set. We also studied the structure of neutron stars for nucleons-only matter with and without K^- condensate in DDRH model using Bonn A set. In this case, the EoS including K^- condensate results in a neutron star having radius < 10 km.

We have compared the results of DDRH model with those of RMF model with GM1 set [9]. The qualitative agreement between the results of these two models is good. Earlier, it was argued that many body correlations may prevent antikaon condensation to occur in neutron stars [11,12]. On the contrary, the study of antikaon condensation in DDRH model with density dependent meson-baryon couplings which take into account many body correlations, shows that it is a possibility in neutron stars. In this calculation, we have treated meson-(anti)kaon couplings as constant. In principle, one may consider density dependent meson-(anti)kaon couplings. This will introduce additional rearrangement term in the antikaon sector. It will be reported in a future publication.

REFERENCES

- [1] N. K. Glendenning, Compact stars, (Springer, New York, 1997).
- [2] D.B. Kaplan and A.E. Nelson, Phys. Lett. B **175**, 57 (1986);
A.E. Nelson and D.B. Kaplan, Phys. Lett. B **192**, 193 (1987).
- [3] M. Hanauske, D. Zschesche, S. Pal, S. Schramm, H. Stöcker and W. Greiner, Astrophys. J **537**, 958 (2000).
- [4] M. Prakash, I. Bombaci, M. Prakash, Paul J. Ellis, J. M. Lattimer and R. Knorren, Phys. Rep. **280**, 1 (1997).
- [5] J. Schaffner and I.N. Mishustin, Phys. Rev. C **53**, 1416 (1996).
- [6] R. Knorren, M. Prakash and P.J. Ellis, Phys. Rev. C **52**, 3470 (1995).
- [7] N.K. Glendenning and J. Schaffner-Bielich, Phys. Rev. Lett. **81**, 4564 (1998);
N.K. Glendenning and J. Schaffner-Bielich, Phys. Rev. C **60**, 025803 (1999).
- [8] S. Pal, D. Bandyopadhyay and W. Greiner, Nucl. Phys. **A674**, 553 (2000);
S. Banik and D. Bandyopadhyay, Phys. Rev. C **63**, 035802 (2001).
- [9] S. Banik and D. Bandyopadhyay, Phys. Rev. C **64**, 055805 (2001).
- [10] U.H. Gerlach, Phys. Rev. **172**, 1325 (1968).
- [11] V.R. Pandharipande, C.J. Pethick and V. Thorsson, Phys. Rev. Lett. **75**, 4567 (1995).
- [12] J. Carlson, H. Heiselberg and V.R. Pandharipande, Phys. Rev. C **63**, 017603 (2001).
- [13] R.B. Wiringa, V. Fiks and A. Fabrocini, Phys. Rev. C **38**, 1010 (1988).
- [14] A. Akmal, V. Pandharipande and D.G. Ravenhall, Rev. C **58**, 1804 (1998).
- [15] B. D. Serot and J. D. Walecka, Ad. Nucl. Phys. **16**, 1 (1986);
J. D. Walecka, Theoretical Nuclear and Subnuclear Physics (Oxford , Oxford University).
- [16] R. Brockmann and H. Toki, Phys. Rev. Lett. **68**, 3408 (1992).
- [17] C. Fuchs, H. Lenske and H.H. Wolter, Phys. Rev. C **52**, 3043 (1995).
- [18] H. Lenske and C. Fuchs, Phys. Lett. B **345**, 355 (1995).
- [19] M.R. Anastasio, L.S. Celenza, W.S. Pong and C.M. Shakin, Phys. Rep. **100**, 327 (1983).
- [20] C.J. Horowitz and B.D. Serot, Nucl. Phys. **A464**, 613 (1987).
- [21] B. Ter Haar and R. Malfliet, Phys. Rep. **149**, 207 (1987).
- [22] R. Machleidt, Adv. Nucl. Phys. **19**, 189 (1989).
- [23] R. Brockmann and R. Machleidt, Phys. Rev. C **42**, 1965 (1990).
- [24] H.F. Boersma and R. Malfliet, Phys. Rev. C **49**, 233 (1994).
- [25] H. Huber, F. Weber and M.K. Weigel, Phys. Rev. C **51**, 1790 (1995).
- [26] F. de Jong and H. Lenske, Phys. Rev. C **57**, 3099 (1998).
- [27] H. Mütter, M. Prakash and T.L. Ainsworth, Phys. Lett. B **199**, 469 (1987).
- [28] L. Engvik, M. Hjorth-Jensen, E. Osnes, G. Bao and E. Ostgaard, Phys. Rev. Lett. **73**, 2650 (1994).
- [29] H. Huber, F. Weber, M.K. Weigel and C. Schaab, Int. J. Mod. Phys. E **7**, 301 (1998).
- [30] S. Haddad and M. Weigel, Phys. Rev. C **48**, 2740 (1993).
- [31] M.L. Cescato and P. Ring, Phys. Rev. C **57**, 134 (1998).
- [32] S. Typel and H.H. Wolter, Nucl. Phys. **A656**, 331 (1999).
- [33] C.M. Keil, F. Hofmann and H. Lenske, Phys. Rev. C **61**, 064309 (2001).
- [34] F. Hofmann, C.M. Keil and H. Lenske, Phys. Rev. C **64**, 034314 (2001).
- [35] T. Nikšić, D. Vretenar, P. Finelli and P. Ring, nucl-th/0205009.
- [36] F. Hofmann, C.M. Keil and H. Lenske, Phys. Rev. C **64**, 025804 (2001).

- [37] N.K. Glendenning, Phys. Rev. D **46**, 1274 (1992).
- [38] F. de Jong and H. Lenske, Phys. Rev. C **58**, 890 (1998).
- [39] R. Malfliet, Prog. Part. Nucl. Phys. **21**, 207 (1988).
- [40] C.B. Dover and A. Gal, Prog. Part. Nucl. Phys. **12**, 171 (1985).
- [41] J. Haidenbauer, W. Melnitchouk and J. Speth, nucl-th/9805014.
- [42] R.E. Chrien and C.B. Dover, Annu. Rev. Nucl. Part. Sci. **39**, 113 (1989).
- [43] T. Fukuda et al., Phys. Rev. C **58**, 1306 (1998).
- [44] P. Khaustov et al., Phys. Rev. C **61**, 054603 (2000).
- [45] S. Bart et al., Phys. Rev. Lett. **83**, 5238 (1999).
- [46] E. Friedman, A. Gal and C.J. Batty, Nucl. Phys. **A579**, 518 (1994);
C.J. Batty, E. Friedman and A. Gal, Phys. Rep. **287**, 385 (1997).
- [47] G.Q. Li, C.-H. Lee and G.E. Brown, Phys. Rev. Lett. **79**, 5214 (1997); Nucl. Phys. **A625**, 372 (1997).
- [48] S. Pal, C.M. Ko, Z. Lin and B. Zhang, Phys. Rev. C **62**, 061903(R) (2000).
- [49] V. Koch, Phys. Lett. B **337**, 7 (1994).
- [50] T. Waas and W. Weise, Nucl. Phys. **A625**, 287 (1997).
- [51] M. Lutz, Phys. Lett. B **426**, 12 (1998).
- [52] A. Ramos and E. Oset, Nucl. Phys. **A671**, 481 (2000).
- [53] J. Schaffner-Bielich, V. Koch and M. Effenberger, Nucl. Phys. **A669**, 153 (2000).
- [54] A. Cieplý, E. Friedman, A. Gal and J. Mareš, Nucl. Phys. **A696**, 173 (2001).
- [55] E. Friedman, A. Gal, J. Mareš and A. Cieplý, Phys. Rev. C **60**, 024314 (1999).
- [56] G. Baym, C.J. Pethick and P. Sutherland, Astrophys. J. **170**, 299 (1971).
- [57] J.W. Negele and D. Vautherin, Nucl. Phys. **A207**, 298 (1974).

TABLES

TABLE I. Density dependent meson-nucleon couplings at saturation density are obtained from DB calculations using Groningen nucleon-nucleon potential in Ref. [34]. Infinite nuclear matter properties calculated with momentum corrected meson-nucleon vertices are binding energy $E/A = -15.6$ MeV, saturation density $n_0 = 0.18 fm^{-3}$, asymmetry energy coefficient $a_{asy} = 26.1$ MeV, incompressibility $K = 282$ MeV and effective nucleon mass $m_N^*/m_N = 0.554$. Masses for nucleons and mesons are $m_N = 939$ MeV, $m_\sigma = 550$ MeV, $m_\omega = 783$ MeV and $m_\rho = 770$ MeV. The parameterization of density dependent σ and ω -nucleon couplings for Bonn A potential is taken from Ref. [30,31]. The nuclear matter properties in Bonn A potential are $E/A = -15.75$ MeV, $n_0 = 0.159 fm^{-3}$, $a_{asy} = 34.3$ MeV, $K = 151.3$ MeV and $m_N^*/m_N = 0.642$. All hadronic masses for Bonn A case are same as in Groningen case. The ρ meson-nucleon coupling is density independent and no δ meson is present in Bonn A case. All parameters are dimensionless.

	$g_{\sigma N}$	$g_{\omega N}$	$g_{\rho N}$	$g_{\delta N}$
Groningen	9.9323	12.1872	5.6200	7.6276
Bonn A	9.5105	11.5401	8.0758	-

TABLE II. Scaling factor for σ and ω meson-hyperon vertices for Groningen and Bonn A nucleon-nucleon potential.

	$R_{\sigma\Lambda}$	$R_{\omega\Lambda}$	$R_{\sigma\Xi}$	$R_{\omega\Xi}$
Groningen	0.5218	0.49	0.3104	1/3
Bonn A	0.4911	0.49	0.3343	1/3

TABLE III. The coupling constants for antikaons (\bar{K}) to σ -meson, $g_{\sigma K}$, for various values of \bar{K} optical potential depths $U_{\bar{K}}(n_0)$ (in MeV) at saturation density. The results are for Groningen and Bonn A nucleon-nucleon potential.

$U_{\bar{K}}(n_0)$	-120	-140	-160	-180
Groningen	0.1993	0.6738	1.1483	1.6228
Bonn A	1.1121	1.6609	2.2097	2.7585

TABLE IV. The maximum masses M_{max} and their corresponding central densities $u_{cent}=n_{cent}/n_0$ for nucleon-only (np) star matter and for stars with further inclusion of hyperons (np Λ (Ξ)) are given below. The results are for Groningen set. The threshold densities for K^- and \bar{K}^0 condensation, $u_{cr}(K^-)$ and $u_{cr}(\bar{K}^0)$ where $u = n_B/n_0$ and also M_{max} and u_{cent} for neutron star matter including Λ hyperons at different values of antikaon optical potential depth $U_{\bar{K}}(n_0)$ (in MeV) at saturation density are given. The values in the parentheses are those of neutron star matter including Ξ .

	$U_{\bar{K}}(n_0)$	$u_{cr}(K^-)$	$u_{cr}(\bar{K}^0)$	u_{cent}	M_{max}/M_\odot
np	-	-	-	5.11	2.313
np Λ (Ξ)		-	-	5.13 (4.89)	1.708 (1.620)
np $\bar{K}\Lambda$ (Ξ)	-120	3.83 (-)	- (-)	4.84 (4.89)	1.697 (1.620)
	-140	3.17 (5.74)	7.27 (7.39)	4.56 (4.89)	1.665 (1.620)
	-160	2.65 (3.20)	6.16 (6.16)	4.38 (4.49)	1.602 (1.599)
	-180	2.28 (2.29)	5.16 (5.16)	5.16 (5.16)	1.497 (1.497)

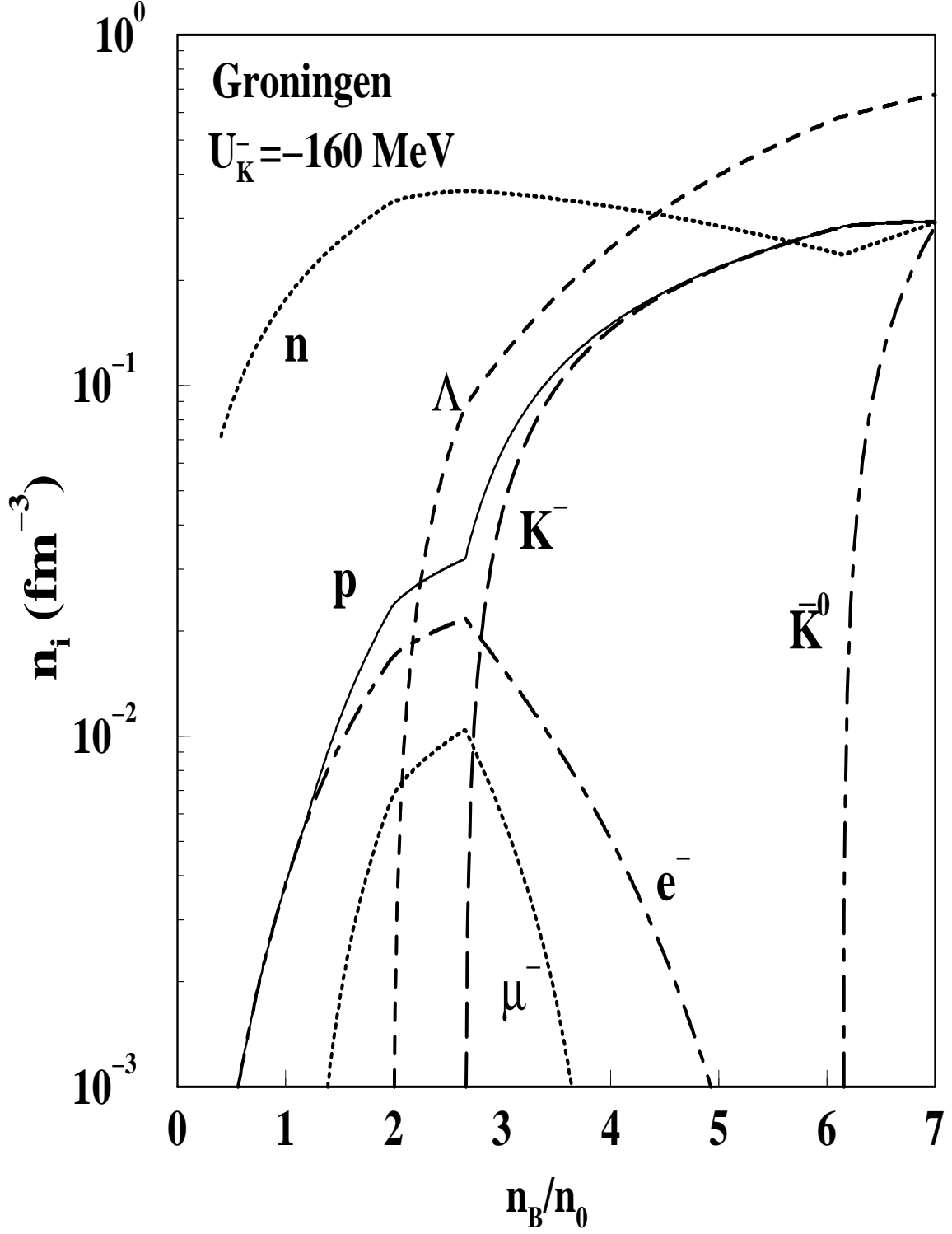


FIG. 1. Number densities (n_i) of various particles in β -equilibrated n,p, Λ and lepton matter including K^- and \bar{K}^0 condensate for Groningen set and antikaon optical potential depth at normal nuclear matter density $U_{\bar{K}}(n_0) = -160$ MeV as a function of normalised baryon density.

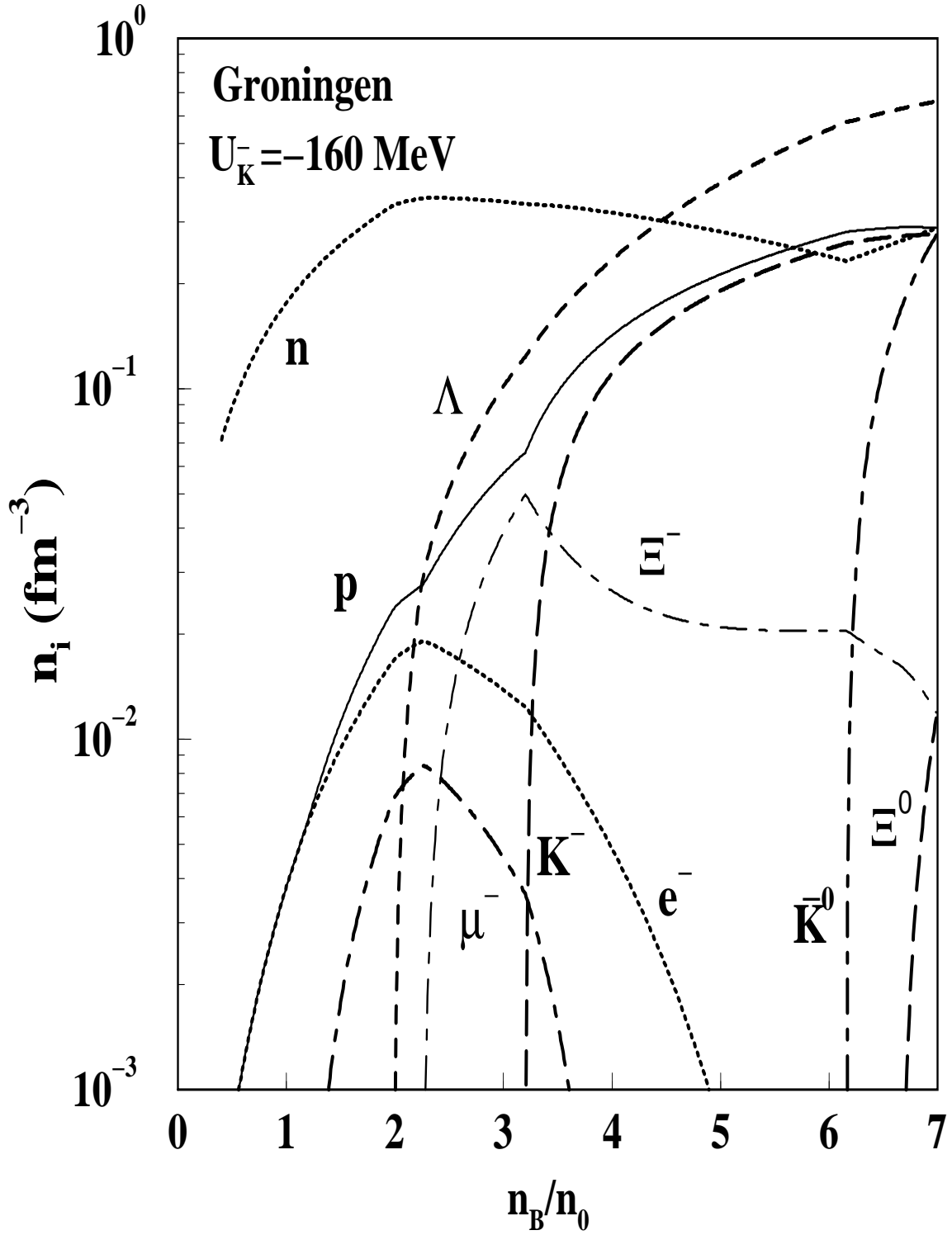


FIG. 2. Number densities (n_i) of various particles in β -equilibrated n, p, Λ, Ξ and lepton matter including K^- and \bar{K}^0 condensate for Groningen set and antikaon optical potential depth at normal nuclear matter density $U_{\bar{K}}(n_0) = -160 \text{ MeV}$ as a function of normalised baryon density.

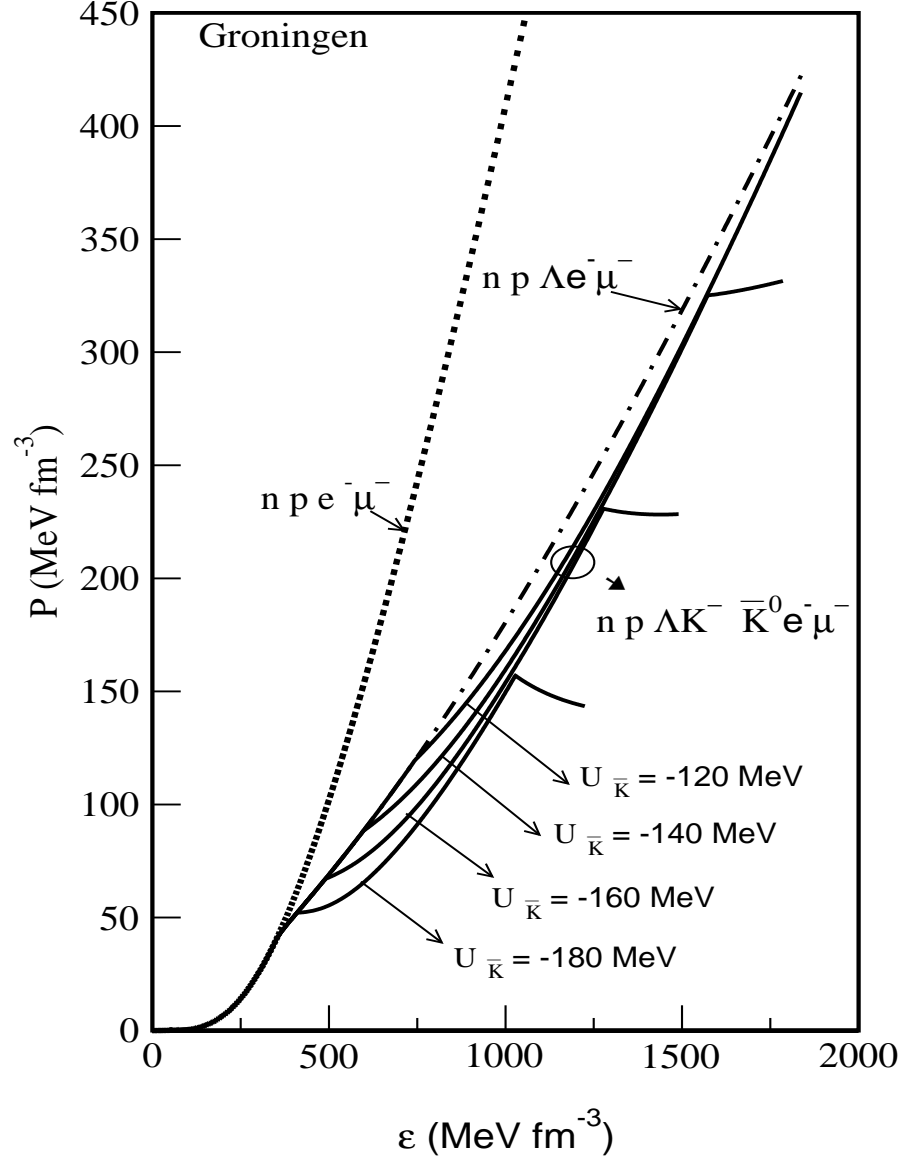


FIG. 3. The equation of state, pressure P vs. energy density ε for Groningen set is shown here. The results are for n,p and lepton matter (dotted line), n,p, Λ and lepton matter (dash-dotted line), and n,p, Λ and lepton matter including K^- and \bar{K}^0 condensate (solid lines) calculated with antikaon optical potential depth at normal nuclear matter density of $U_{\bar{K}}(n_0) = -120, -140, -160, -180$ MeV.

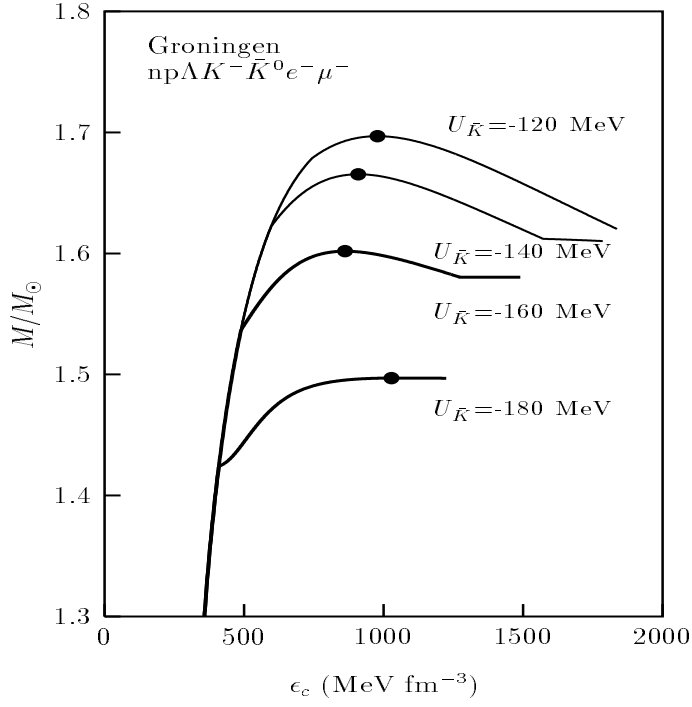


FIG. 4. The compact star mass sequences are plotted with central energy density for Groningen set and antikaon optical potential depth of $U_{\bar{K}}(n_0) = -120, -140, -160, -180$ MeV. The star masses of n,p, Λ and lepton matter with K^- and \bar{K}^0 condensate are shown here.

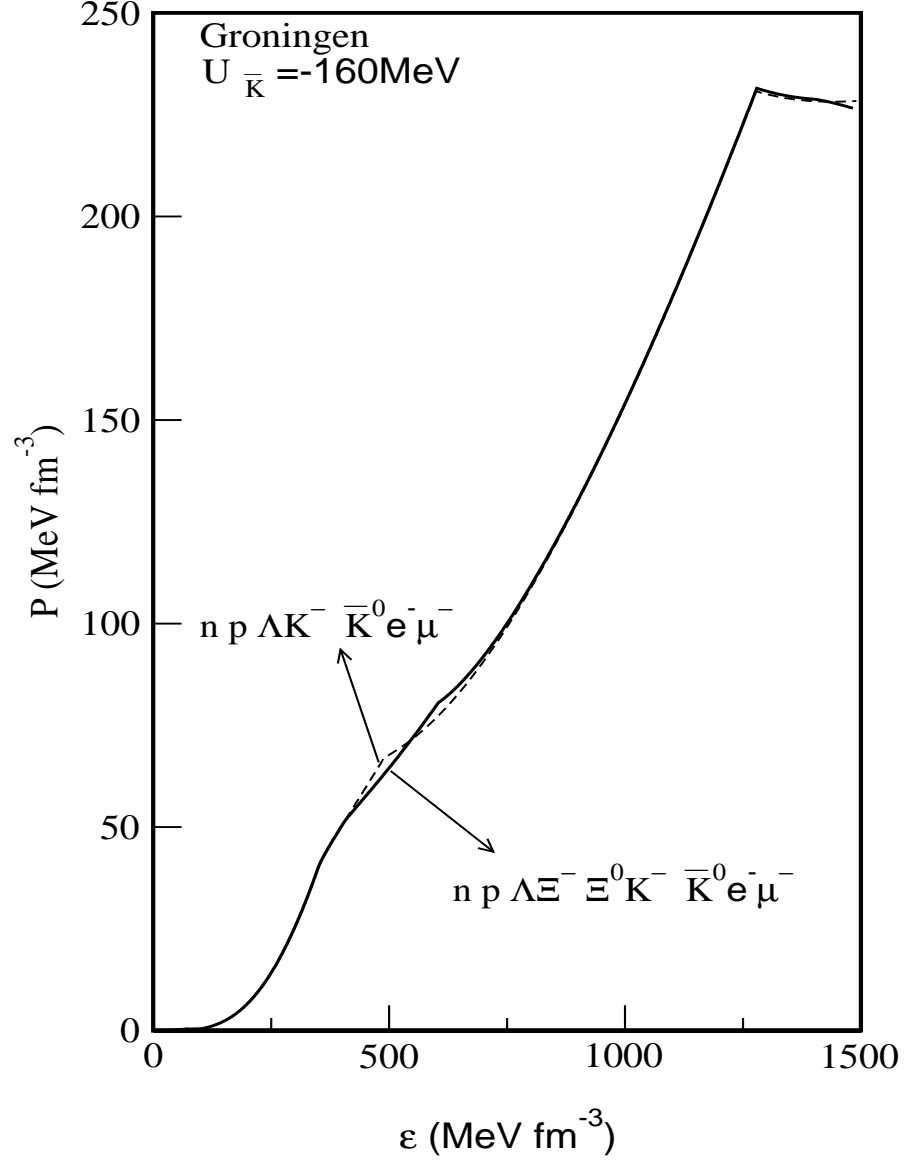


FIG. 5. The equation of state for n, p, Λ, Ξ , lepton and \bar{K} matter (solid line) and n, p, Λ , lepton and \bar{K} matter (dashed lines) calculated with Groningen set and antikaon optical potential depth at normal nuclear matter density of $U_{\bar{K}}(n_0) = -160 \text{ MeV}$ are shown.

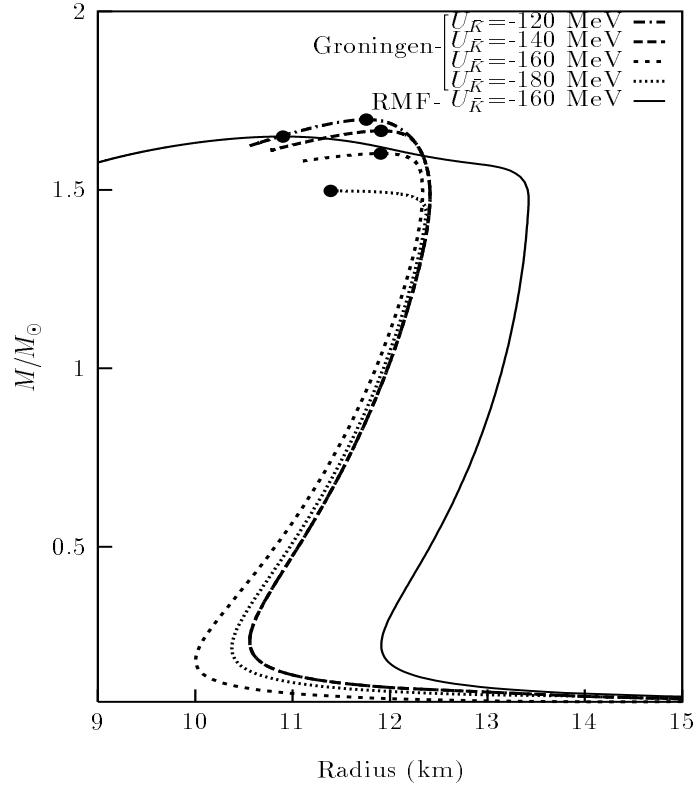


FIG. 6. The mass-radius relationship for compact star sequences for n,p, Λ and lepton matter with K^- and \bar{K}^0 condensate for Groningen set and antikaon optical potential depth of $U_{\bar{K}}(n_0) = -120, -140, -160, -180$ MeV. The mass-radius relationship for compact star sequence for hyperon matter including K^- condensate in the RMF model calculation (Ref. [9]) is also shown here.

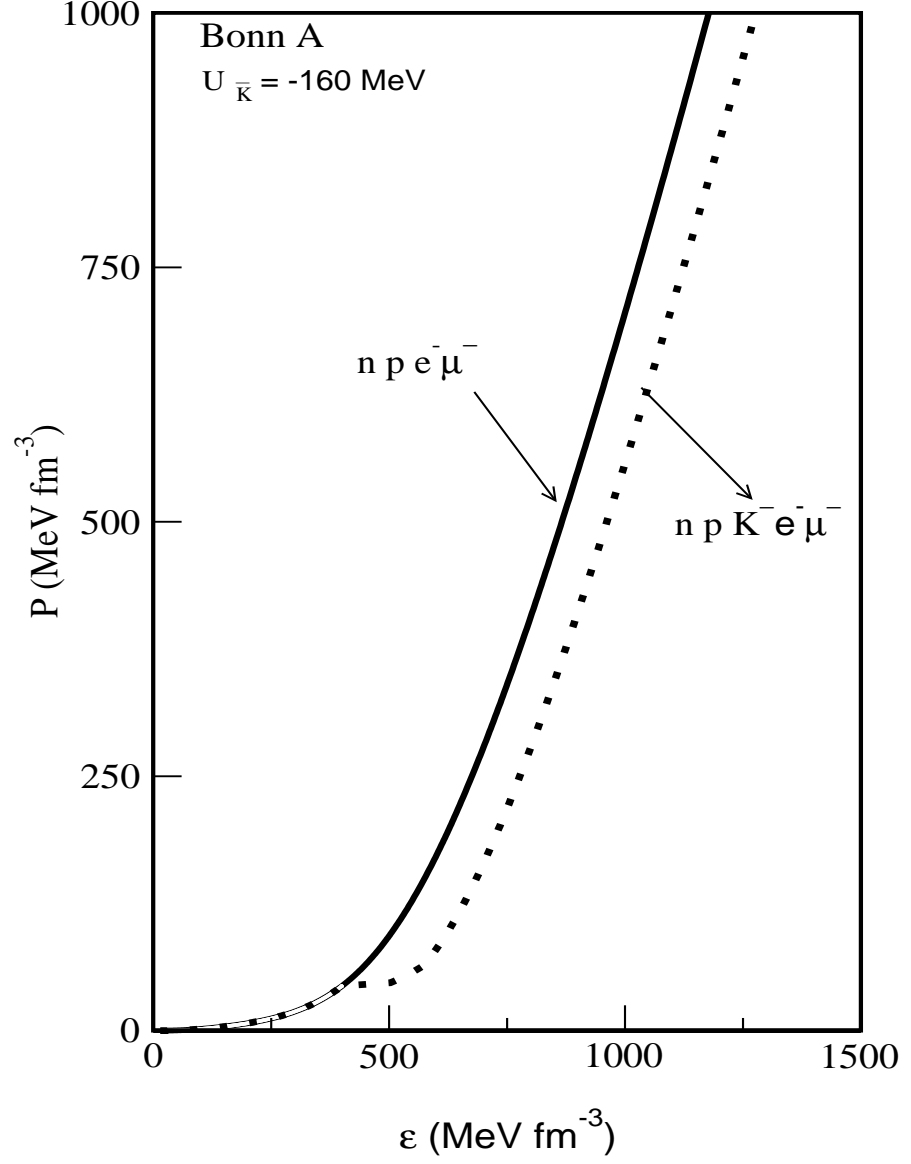


FIG. 7. The equation of state for n,p and lepton matter (solid line) and n,p, lepton and K^- matter (dotted line) calculated with Groningen set and antikaon optical potential depth at normal nuclear matter density of $U_{\bar{K}}(n_0) = -160 \text{ MeV}$ are shown.